

Multi-view Spectral Polarization Propagation for Video Glass Segmentation (Supplementary Material)

Anonymous ICCV submission

Paper ID 6969

This supplementary document provides more details of the proposed PGV-117 dataset (§ 1), the formal definitions of the four quantitative metrics (§ 2), and the detailed calculation of key affinity (§ 3). Five processed video sequences are provided along with this document. The teaser and the visual results shown in section 5.2 of this submission are from these five videos. We also offer additional video results through [Google Drive](#).

1. PGV-117 Dataset

The ground truth masks of the proposed PGV-117 dataset are annotated by annotation professionals, resulting in 144, 686 glass masks. Each ground truth mask is manually checked to ensure the quality of the annotations.

The proposed dataset consists of 117 sequences and 21, 485 frames. The training set offers 85 sequences, 15, 838 frames, and the testing set provides 32 sequences, 5, 647 frames. [Figure 1](#) and [Figure 2](#) show the number of frames for each sequence in the training and testing set, respectively.

2. Formal Definition of Evaluation Metrics

We adopt the four metrics used by Mei *et al.* [5] for evaluating all competing approaches, which are intersection over union (IoU), weighted F-measure (F_β) [4], mean absolute error (MAE), and balance error rate (BER) [6]. Here, we provide the formal definitions of these four metrics.

Intersection over union (IoU)

$$IoU = \frac{\sum_{i=1}^H \sum_{j=1}^W (G(i, j) * P_b(i, j))}{\sum_{i=1}^H \sum_{j=1}^W (G(i, j) + P_b(i, j) - G(i, j) * P_b(i, j))}, \quad (1)$$

where G is the ground truth mask in which the values of the glass region are 1 while those of the non-glass region are 0; P_b is the predicted mask binarized with a threshold of 0.5; and H and W are the height and width of the ground truth mask, respectively.

Weighted F-measure (F_β) takes a prediction map's precision and recall into account, which is a common metric used in salient object detection tasks. Based on recent studies [2, 3], the weighted F-measure [4] is more reliable than the traditional F_β [5], and it is used in our evaluation.

Mean Absolute Error (MAE) calculates the element-wise distance between a prediction map P and the corresponding ground truth mask G :

$$MAE = \frac{1}{H \times W} \sum_{i=1}^H \sum_{j=1}^W |P(i, j) - G(i, j)| \quad (2)$$

where $P(i, j)$ indicates the predicted probability score at location (i, j) .

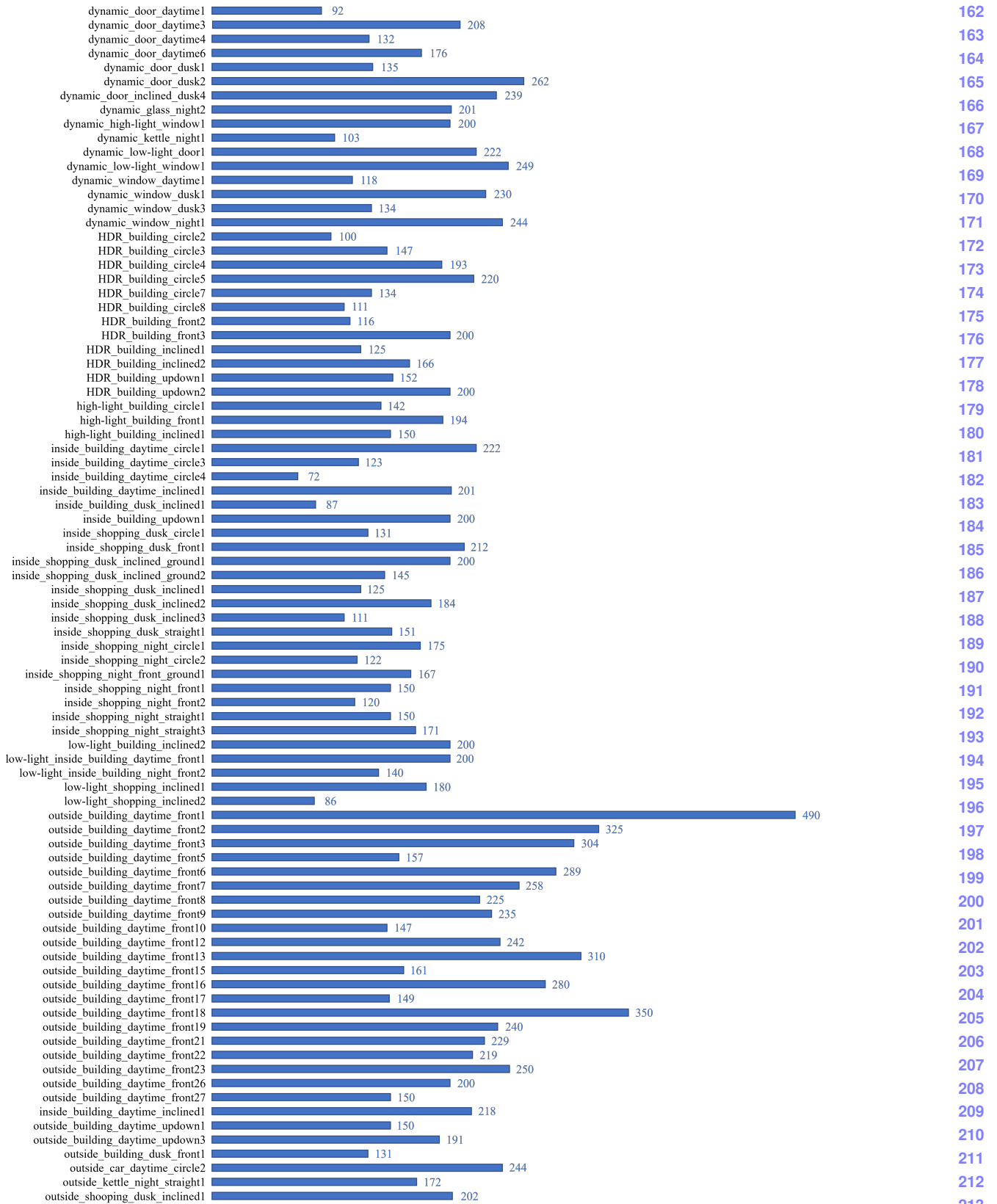


Figure 1. Summary for training set distribution of PGV-117, which includes 85 video sequences in total.

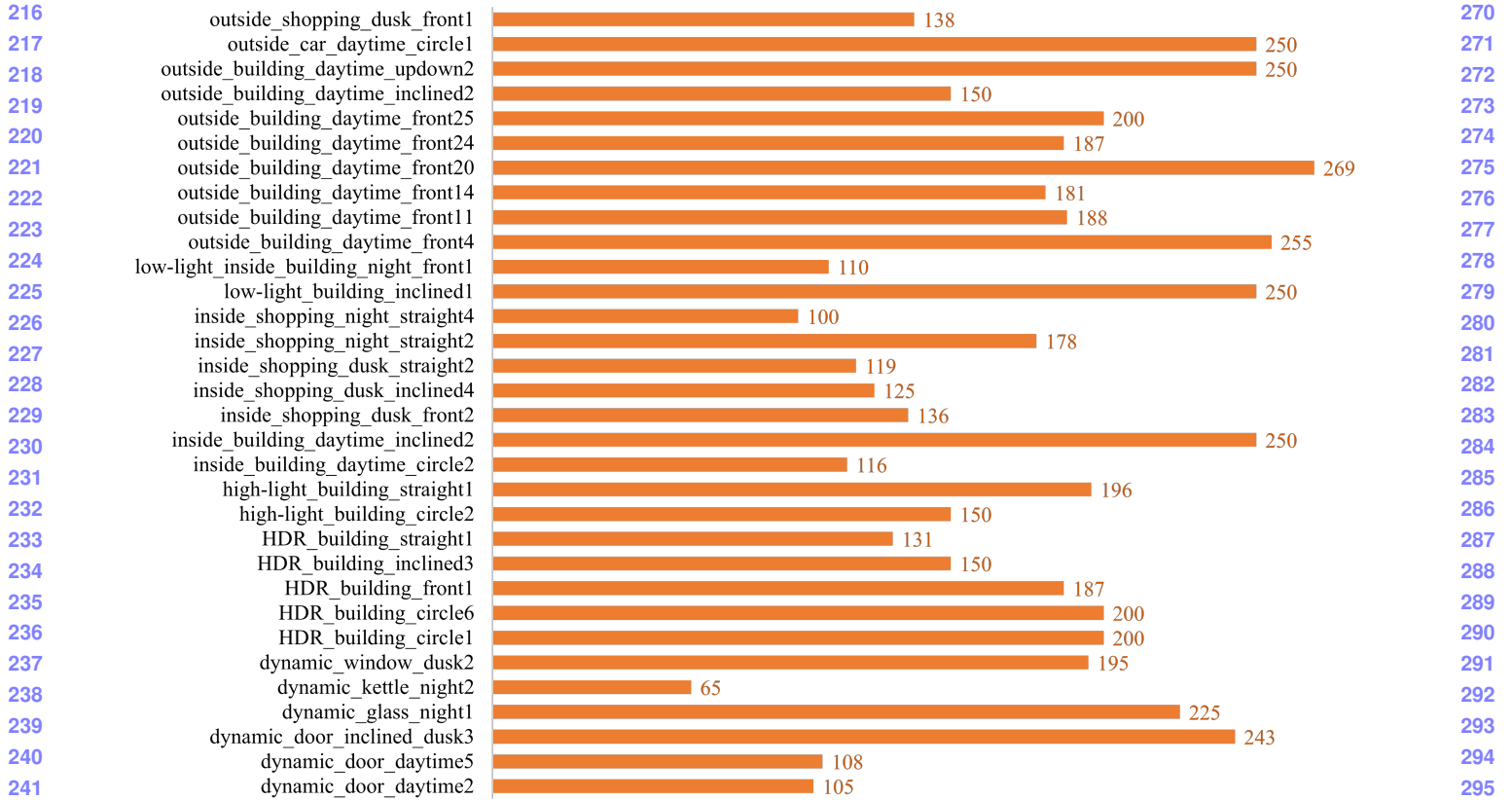


Figure 2. Summary for testing set distribution of PGV-117, which includes 32 video sequences in total. In order not to lose generality, all lighting conditions, camera motion patterns, and dynamics are also included in the testing set.

Balance error rate (BER) is a common metric used in shadow detection tasks. Formally, it is defined as:

$$BER = (1 - \frac{1}{2}(\frac{TP}{N_p} + \frac{TN}{N_n})) \times 100 \quad (3)$$

where TP , TN , N_p , and N_n represent the numbers of true positive pixels, true negative pixels, glass pixels, and non-glass pixels, respectively.

3. Computing Affinity

For the query frame t , we relate multi-view RGB-P information by exploring the relationship between the PGI key of t with the keys in the memory (0 to $t - 1$). After generating the query key k^Q and memory keys k^M , we refer to [7, 1] to calculate the affinity between k^Q and k^M :

$$\begin{aligned} a &= \xi[(k^M)^2], \\ b &= 2 * [(k^M)^T \otimes k^Q], \\ A &= (-a + b) / \sqrt{CK}, \\ A &= \frac{\exp(A_{ij})}{\sum_n (\exp(A_{nj}))}. \end{aligned} \quad (4)$$

where $\xi[\cdot]$ represents the summation and unsqueeze operation, \otimes means matrix multiplication. CK is the number of channels for the key features, and i denotes the affinity value at the i -th position. The affinity considers both RGB similarity and multi-view spectral consistency between the query and memory frames. The value encoder output v^M corresponding to k^M contains features from the tripartite memory values, and the multiplication of affinity and v^M correlates the query frame and historical information to obtain v^Q to participate in the readout of the memory bank.

324
325
326
327
328
329
330
331
332
333
334
335
336
337
338
339
340
341
342
343
344
345
346
347
348
349
350
351
352
353
354
355
356
357
358
359
360
361
362
363
364
365
366
367
368
369
370
371
372
373
374
375
376
377

References

[1] Ho Kei Cheng, Yu-Wing Tai, and Chi-Keung Tang. Rethinking space-time networks with improved memory coverage for efficient video object segmentation. In *NeurIPS*, 2021. 3

[2] Deng-Ping Fan, Ming-Ming Cheng, Yun Liu, Tao Li, and Ali Borji. Structure-measure: A new way to evaluate foreground maps. In *ICCV*, 2017. 1

[3] Deng-Ping Fan, Cheng Gong, Yang Cao, Bo Ren, Ming-Ming Cheng, and Ali Borji. Enhanced-alignment measure for binary foreground map evaluation. In *IJCAI*, 2018. 1

[4] Ran Margolin, Lih Zelnik-Manor, and Ayellet Tal. How to evaluate foreground maps? In *CVPR*, 2014. 1

[5] Haiyang Mei, Bo Dong, Wen Dong, Jiayi Yang, Seung-Hwan Baek, Felix Heide, Pieter Peers, Xiaopeng Wei, and Xin Yang. Glass segmentation using intensity and spectral polarization cues. In *CVPR*, 2022. 1

[6] Vu Nguyen, Tomas F Yago Vicente, Maozheng Zhao, Minh Hoai, and Dimitris Samaras. Shadow detection with conditional generative adversarial networks. In *ICCV*, 2017. 1

[7] Seoung Wug Oh, Joon-Young Lee, Ning Xu, and Seon Joo Kim. Video object segmentation using space-time memory networks. In *ICCV*, 2019. 3

378
379
380
381
382
383
384
385
386
387
388
389
390
391
392
393
394
395
396
397
398
399
400
401
402
403
404
405
406
407
408
409
410
411
412
413
414
415
416
417
418
419
420
421
422
423
424
425
426
427
428
429
430
431